TECHNICAL PAPER

Statistical modes method—SMM for vibroacoustics calculations of coupled systems

Bruno de Castro Braz[1] · Carlos D'Andrade Souto[2]

Abstract

Evaluating the vibroacoustic response of a fluid–structure coupled system is a relevant issue in many branches of engineering. Tasks related to this field are the analysis of the acoustic environment of the passenger compartment of a vehicle (in the automotive sector) and estimation of the vibrations of a satellite during its launch (in the aerospace sector). Vibroacoustic response is usually calculated by using the finite element method (FEM) for lower frequency band. For higher frequency band, the statistical energy analysis (SEA) is the usual choice. In this sense, the lack of a method capable to capture the response of the mid-frequency zone or even the full band is a matter of great interest for researchers from the last decades. A novel analytical model to evaluate the full band vibroacoustic response of a coupled system in a simplified way with average response is presented, the statistical modes method (SMM). The SMM provides the maximum responses on each frequency band and the overall response through the integral over the frequency domain. The eigenvalues are calculated based on modal density equations updated to also work in fundamental frequencies, the eigenvectors are not calculated in order to keep the method simple, and however, the variables which need it as coupling factor and nodal forces are analytically approximated from geometrical information and mode number. The method is validated over analytical, FEM, SEA and experimental results. The satellite Amazonia 1 from Instituto Nacional de Pesquisas Espacias acoustic tests was used for the experimental validation.

Keywords Vibroacoustics · Vibrations · Acoustics · Satellite

1 Introduction

The vibroacoustic coupling is a common problem faced by engineering with a wide variety of problems ranging from acoustic comfort within the interior of cars, buildings and airplanes; to the vibration of satellites during its launch. The standard methods to analyze vibroacoustics are finite element method (FEM) for lower frequencies and statistical energy analysis (SEA) for higher frequencies. The FEM main issue in higher frequencies is related to the amount of elements necessary for a proper description of the modes. As a rule of thumb, it is considered necessary about 5–10 elements per wavelength. This leads to a large increase in the number of degrees of freedom, which also greatly increases the computational cost (processing time, memory). Unlike the FEM, the SEA method is based on the average values of the vibrational energy exchanged between parts (subsystems) of the analyzed system. It is considered that the energy exchange takes place between the natural modes of vibration of the subsystems involved. The energy of each subsystem is assumed to be evenly distributed across the modes within the system in the same frequency band. Therefore, SEA needs a high modal density to attend its requirements, and this is the real high frequency sense for SEA. The lack of a method capable to cover the mid-frequency range or even the full range motivated the creation of several studies and methods over the past years. Desmet et al. [1] presented a project with the compilation of the most recent works in the mid-frequency area.

✉ Bruno de Castro Braz
bruno.braz@inpe.br

Carlos D'Andrade Souto
soutocds@fab.mil.br

1 National Institute of Space Research, São José Dos Campos, SP 12227-010, Brazil

2 Institute of Aeronautics and Space, São José Dos Campos, SP 12228-904, Brazil

Hybrid methods coupling FEM and SEA to attend the mid-frequency range were developed, as presented by Langley and Cordioli [2], other works performing this technic are Pirk and Souto [3] and Jiao et al. [4]. Desmet [5] and Desmet et al. [6] proposed the wave-based method (WBM), which is derived from indirect Trefftz method, where a series of functions that are solution of the wave equation are weighted to solve the boundary conditions. The WBM solution requires full matrices that are much smaller than FEM ones, but are frequency dependent and have some difficulties to be implemented in complex geometries. In order to overcome the geometrical issues, Hal et al. [7] and Vanmaele [8] proposed the hybrid method FEM-WBM, the complex geometries are modeled with FEM and the most part of the domain is modeled with WBM to take advantage on the smaller matrices of this method; however, as in WBM, the matrices are also frequency dependent. Another interesting method developed for the mid-frequency context is the statistical model energy distribution analyses (SmEdA), as can be checked on Stelzer [9] and Stelzer et al. [10], the SmEdA is a method direct derived from SEA that consists of the energy exchanges between vibration modes, what solves the SEA issue related to the lower frequencies, however, requires the computation of the eigenvalues and eigenvectors, which tends to be solved by FEM. Other works that present vibroacoustics analysis and experimental data are Braz and Souto [11], Anvariyeh et al. [12] and Zhong et al. [13].

It seems clear that the available models cannot deal with the full range of frequencies and the enhancements proposed for the mid-frequency range require the use of FEM or something similar, which are susceptible to the FEM-related issues. In this context, a novel model that can handle the full range band and keeps simplicity compatible with SEA seems to attend an important demand in vibroacoustic area.

The present work proposes a novel analytical model named as statistical modes method (SMM) with the objective to calculate in a simplified way the maximum response on each spectral band and the overall response given by the integral of the variables over the frequency range of a coupled vibroacoustic problem. These two outputs from the SMM are the most important information required for the design and tests of a system under a vibroacoustic environment. The SMM is based on the estimation of the eigenvalues using modal density equations, and therefore, the statistical properties of the SEA are also used in SMM to describe a behavior that in average corresponds to the real one. In order to keep the method simple, the eigenvectors are not evaluated, and a special analytical treatment is applied for the variables which need it. As the SMM is based on eigenvalues, the coupled system is solved through modal summation, then the modal analysis may demand matrix inverse operations. If the fluid used has lower density, as the case of air, the SMM provides the calculation of coupling resistances which decouple the equations but keeps the mutual influence between fluid and structure. Stelzer [9] and Fahy [14] mentioned that the modal density would be used for eigenvalue determination, and however, no effective data regarding this were found in the literature.

The modal density is a field of research for acoustic engineering since the beginning of twentieth century, as this affects the sound quality of acoustic chambers. Three of the most cited articles in acoustics are from the 40's, the work of Richard Bolt (Bolt [15, 16] and [17]) presented formulas, tables and graphics for the determination of modal density of rectangular acoustic chambers. Schroeder and Kuttruff [18] presented the Schroeder frequency; beyond this frequency a diffuse field and high modal density can be assumed. Bonello [19] and Cox et al. [20] showed the influence of the sound quality in rooms and auditoriums regarding average modal spacing. The development of modal density of structural elements, as bars, beams and plates started mainly motivated by the development of SEA in 60's. The modal density is an important term in SEA formulation and its development can be seen in several works, as Hart and Shah [21], Clarkson and Ranky [22] for sandwich panels and Xie et al. [23] that presents a resume of analytical deductions of several types of elements. All this understanding on acoustics and modal density was paramount for the development of the SMM method.

The SMM was validated by Monte Carlo analysis with 864 interactions of rectangular geometries (analytical solution), by two finite element models with also comparison to SEA in order to verify its behavior for complex geometries and by comparison to results obtained for the Amazonia 1 satellite acceptance acoustic tests in order to verify it against real experimental data. Amazonia 1 satellite is a project from Instituto Nacional de Pesquisas Espaciais (INPE) and was successfully launched by a PSLV launch vehicle on February 28th of 2021, as shown in Fig. 1.

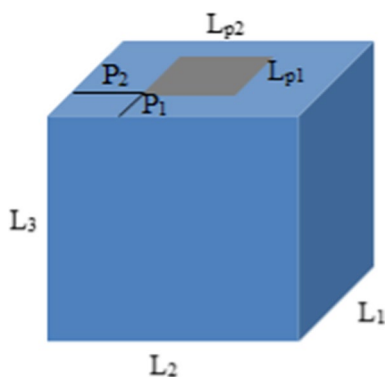**Fig. 1** Amazonia 1 satellite assembled on PSLV fourth stage (*Source*: INPE/ISRO)

Fig. 2 Model used for SMM development, volume sides: L_1, L_2, L_3; plate sides: L_{p1}, L_{p2}; plate position: P_1, P_2

The presented paper contributes to the vibroacoustic discipline with a new analytical model that seems to be capable to solve coupled problems with relative low computational cost and to provide the eigenvalues, maximum responses and overall results, by integrals in frequency domain, in all frequency bands with reasonable accuracy.

2 SMM

The SMM development is divided in eigenvalues estimator, coupling factor, modal force, modal source, modal mass, modal volume and couple modal model.

A simple but representative vibroacoustic system is considered for the analysis and development of the method: a rigid walled regular hexahedral-shaped cavity with a metal plate mounted in one of its walls, as described in Fig. 2.

2.1 Eigenvalue estimator

The SMM eigenvalue estimator was developed based on modal density adapted to also work in fundamental frequencies with a reasonable error.

First, the original density equations presented on Wijker [24] are described, respectively, for simply supported plates and rigid walled volumes

$$N_{\text{plate}} = \frac{k^2 S}{4\pi} - \frac{kP}{4\pi}, \tag{1}$$

$$N_{\text{vol}} = \frac{Vk^3}{6\pi^2} + \frac{S_{\text{total}} k^2}{16\pi} + \frac{P_{\text{vol}} k}{16\pi}, \tag{2}$$

where N is the number of modes, k is the wave number, S is the area, P is the perimeter, and V is the volume.

The adaptation of these equations to be used as a natural frequency estimator for arbitrary geometries involves the use

of a dimensionless wave number (K), the definition of error criteria, the sum of a correction variable α and its adjustment based on an analytical study of rectangular geometries with different aspect ratios.

The rectangular plates considered have aspect ratios varying from 1 to 7 and the rectangular volumes have aspect ratios varying from 1 to 10, but limited to prevent the acoustic cavities to behave like acoustic tubes in, if $R1 = 1$ than $R2 < 4$ and if $R1 = 2$ than $R2 < 7$. The aspect ratios $R1$ and $R2$ can be described as L_2/L_1 and L_3/L_1, see Fig. 2, where L_1 is the smallest side of the volume.

Table 1 presents the error criteria used. The errors defined for the volume may seem to be higher, and however, as the wave number of the volume is directly proportional to the frequency and the plate natural frequencies are proportional to the squared wave numbers, the results are similar. Most of the errors faced by the method are due to degenerate modes, which are modes with same eigenvalue but different eigenvectors, the method is not able to model them with same frequency. Although developed via analysis using rectangular geometries, the average results for complex shapes are in agreement with error criteria. Equations (3) and (4) show the proposed adaptations.

$$k = \frac{K}{\sqrt{S}} \Rightarrow N_{\text{plate}} = \frac{K^2}{4\pi} - \frac{K}{4\pi}\left(\frac{P^2}{S}\right)^{0.5} + K\alpha_p \tag{3}$$

$$k = \frac{K}{V^{1/3}} \Rightarrow N_{\text{vol}} = \frac{K^3}{6\pi^2} + \frac{K^2}{16\pi}\left(\frac{S_{\text{total}}^{1.5}}{V}\right)^{2/3} + K\alpha_v. \tag{4}$$

Plate and volume wavenumber estimator formulas using, respectively, Baskhara and Cardano-Tartaglia are given by

$$k_p = \left[\frac{\frac{1}{4\pi}\sqrt{\left(\frac{P^2}{S}\right)} - \alpha_p + \sqrt{\left(\alpha_p - \frac{1}{4\pi}\sqrt{\left(\frac{P^2}{S}\right)}\right)^2 + \frac{N_{\text{plate}}}{\pi}}}{\frac{1}{2\pi}}\right]\frac{1}{\sqrt{S}}, \tag{5}$$

Table 1 Wave number error criteria for plate and volume eigenvalue estimators

Plate	Volume
Mode 1 < 10%	Mode 2 < 35%
Mode 2 < 11%	Mode 3 < 30%
Mode 3 < 10%	Mode 4 < 30%
Mode 4 < 12%	Mode 5 < 30%
Mode 5 < 13%	Mode 6 < 30%

$$k_v = \left[-\frac{\pi}{8}\left(\frac{S_{total}^{1.5}}{V}\right)^{2/3} + \left[-\frac{q}{2} + \sqrt{\frac{q^2}{4} + \frac{p^3}{27}} \right]^{(1/3)} + \left[-\frac{q}{2} - \sqrt{\frac{q^2}{4} + \frac{p^3}{27}} \right]^{(1/3)} \right] \frac{1}{V^{\frac{1}{3}}} \tag{6}$$

where

$$\alpha_p = 0.2411111 - 0.0063194\left(\frac{P^2}{S}\right) \tag{7}$$

$$p = 6\pi^2\alpha_v - 3\left[\frac{\pi}{8}\left(\frac{S_{total}^{1.5}}{V}\right)^{2/3}\right]^2, \tag{8}$$

$$q = -6\pi^2 N_{vol} - \frac{3\pi^3\alpha_v}{4}\left(\frac{S_{total}^{1.5}}{V}\right)^{2/3} + 2\left[\frac{\pi}{8}\left(\frac{S_{total}^{1.5}}{V}\right)^{2/3}\right]^3, \tag{9}$$

$$\alpha_v = 0.0395842\left(\frac{S^{1.5}}{V}\right) - 0.411767. \tag{10}$$

2.2 Coupling factor

For a volume mode n and a plate mode i, a coupling factor is given by the integral of these modes eigenvectors over the plate area. The SMM works statistically in order to describe the vibroacoustic problem in a simple way; therefore, the eigenvector is not evaluated, and a statistical approach based on average is used. The coupling factor can be approximated as the multiplication of two independent integrals, each one in one dimension of the plate, that is treated independently, according to

$$\int_S \widehat{w}_i\widehat{p}_n dS \cong \int_0^{L_{p1}} \sin\left(\frac{x\pi i}{L_{p1}}\right)\cos\left(\frac{(x+p_x)\pi n}{L_{v1}}\right)dx \int_0^{L_{p2}} \sin\left(\frac{y\pi j}{L_{p2}}\right)\cos\left(\frac{(y+p_2)\pi z}{L_{v2}}\right)dy, \tag{11}$$

where L_p and L_v are the plate and volume length on each direction, p is the plate position on volume, $i,j = 1, 2, 3\ldots$, $n,z = 0, 1, 2\ldots$ and S is the plate area.

In order to deal with arbitrary geometry and different configurations, the average of the first integral of Eq. (11) over plate length L_{p1} (0 to L_{v1}) and position p_1 (0 to L_{v1}-L_{p1}) is taken in Eq. (12). For simplicity, notation $1,2$ referring to plate dimensions will be omitted from now on.

$$\int_0^{L_v}\int_0^{L_v-L_p}\int_0^{L_p} \sin\left(\frac{\pi i}{L_p}x\right)\cos\left(\frac{\pi n}{L_v}(x+p)\right)dx\frac{dp}{L_v-L_p}\frac{dL_p}{L_v} \tag{12}$$

The first two integrals can be analytically solved, which results in

$$\int_0^{L_v-L_p}\int_0^{L_p} \sin\left(\frac{\pi i}{L_p}x\right)\cos\left(\frac{\pi n}{L_v}(x+p)\right)\frac{dxdp}{L_v-L_p} \tag{13}$$

$$= A\sin\left(\frac{\pi n L_p}{L_v}\right)[\cos(\pi n) - \cos(\pi i)],$$

where

$$A = \frac{L_v}{\pi n}\left(\frac{1}{L_v-L_p}\right)\left(\frac{1}{2\left(\frac{\pi n}{L_v} - \frac{\pi i}{L_p}\right)} - \frac{1}{2\left(\frac{\pi n}{L_v} + \frac{\pi i}{L_p}\right)}\right). \tag{14}$$

The last integral was solved with the use of Wolfram Alpha integrator [25] and resulted in an equation dependent of minus Sinc function integrated from x to infinite, which can be approximated by ± 1.5 for $\pm x$ different than 0. Performing all calculations and approximations result in the following

$$\frac{3inL_v}{2\pi^2 n^2(i^2-n^2)}(\cos(\pi n) - \cos(\pi i)), \text{ for } i > n, \tag{15}$$

$$\frac{3i^2 L_v}{2\pi^2 n^2(i^2-n^2)}(\cos(\pi n) - \cos(\pi i)), , \text{ for } n > i \tag{16}$$

and a point of discontinuity for $i = n$.

Now some physical simplifications can be performed in order to produce a practical result that can be applied in the SMM method. First, the L_v is obtained by the integral of L_p over the volume, so in fact, this length is actually regarded

to the plate dimension, $L_v => L_p$. The modes counters i and n can be considered to be in the same order, $n \sim = i$. The relation (i^2-n^2) can be approximated to be in the same order of magnitude than i^2, $(i^2 - n^2) \sim = i^2$. The last approximation concerns to the expression $(\cos(\pi n) - \cos(\pi i))$, which can assume three possible values, 0, 1 or 2, and in average is equal to 1, than this expression is approximate to 1. The wave counters numbers of plates were preferred in relation to the volume ones because volume counters can assume zero value, which make them unstable for practical use.

After some manipulations in Eqs. (15) and (16), the average coupling factor regarding one dimension of the integral of the plate is obtained, however, the SMM looks for the maximum responses over each frequency band, then the expression is multiplied by two twice, one for each average taken, and finally, the expression is multiplied by the result of the other direction, which results in the following final formula

$$\int_S \widehat{p}_n \widehat{w}_i \, dS \cong \frac{0.4S}{(ij)^2}, \tag{17}$$

where S is the plate area, and ij is the multiplication between the wave counters in the two directions of each plate mode. The ij term can also be treated as the quantity of maximum and minimum response for each plate mode eigenvector.

Although Eq. (17) is very simple, the quantity ij cannot be calculated analytically and because of that a simplification based on the study of rectangular plates is used according to Fig. 3 and Eq. (18).

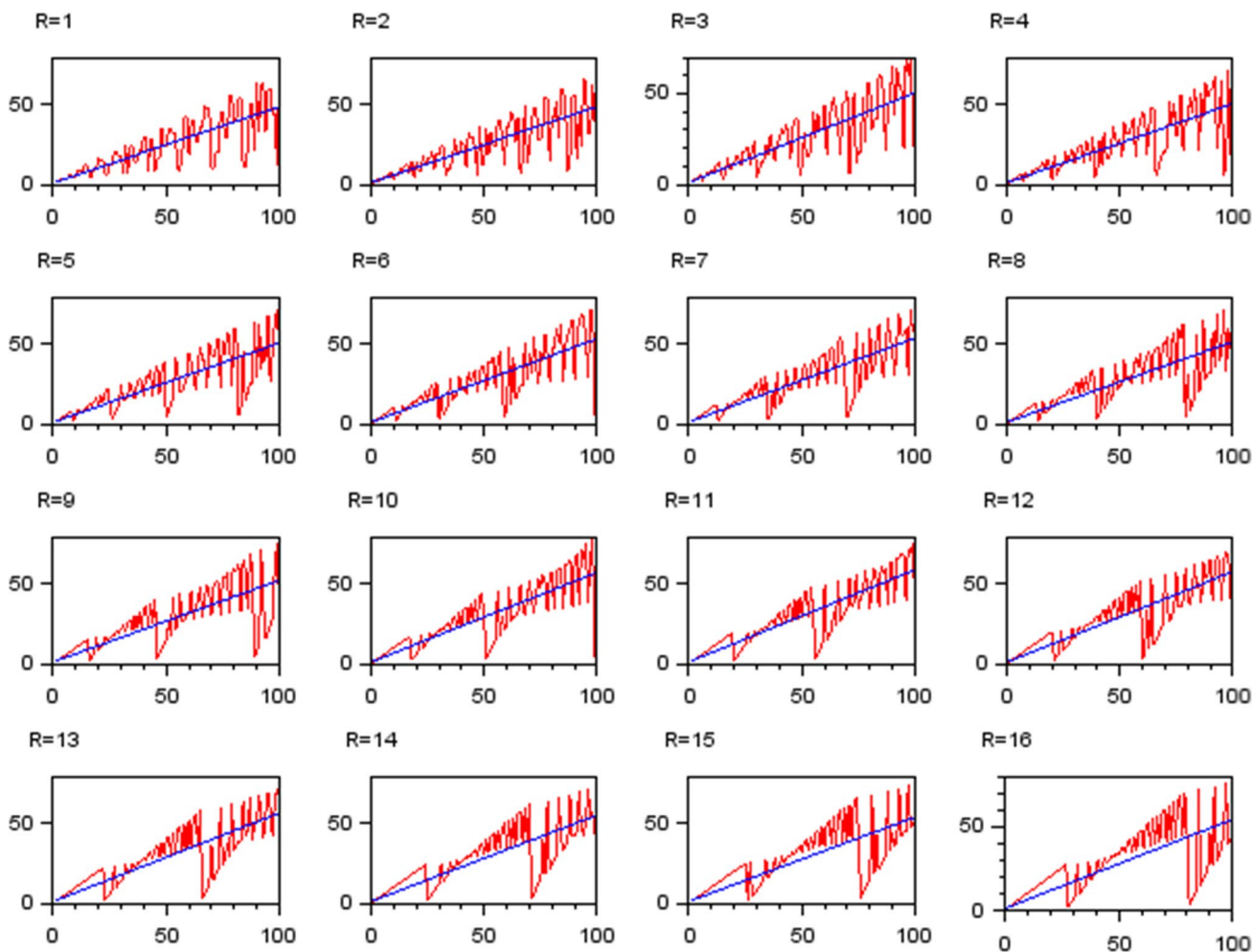$$ij \cong 1 + 0.5N, \quad ij = 1 \text{ for } N = 1. \tag{18}$$

Fig. 3 ij relation for plates with aspect ratio R from 1 to 16 (The horizontal axis is the mode number, the vertical axis is the ij, the red line is the actual result, and the blue line is Eq. (18))

Equation (17) represents a huge simplification in the coupling factor. The final value depends only on the plate area S and mode number N. Studies comparing this result with the calculation of the real integral show that, on average, this expression can be considered valid.

2.3 Nodal force

The modal force of a nodal input in a simply supported plate is dependent on the mass (M_p) and the eigenvector value on the nodal position (px, py) and can be expressed as:

$$F_{m\_i} = \frac{\int_S P\delta(px, py)\hat{w}_i \mathrm{d}s}{\rho \int_S \hat{w}_i \hat{w}_i \mathrm{d}s} = \frac{4F\hat{w}_i(px, py)}{M_p}. \tag{19}$$

It is clear from Eq. (19) that is necessary an approximation for the eigenvector value for the use of this expression on SMM. Considering again a rectangular plate, it is possible to describe the eigenvector as the multiplication of two sines with the phase of the nodal position of the first mode multiplied by its wave counter, then, taking advantage of

Eq. (18), the value of the eigenvector in a determined position can be approximated by

$$\hat{w}(x, y) = \sin\left(\frac{i\pi x}{L_x}\right)\sin\left(\frac{j\pi y}{L_y}\right)$$
$$= \sin(i\varphi_1)\sin(j\varphi_2) \cong \sin(ij\varphi_{1\,\mathrm{mod}}). \tag{20}$$

In a rectangular plate one of the phases φ_1 and φ_2 will have the value of $\pi(1 - R_c)/2$ and the other phase value will lie in the range between $\pi/2$ and $\pi(1 - R_c)/2$, where R_c is the ratio of the distance connecting the plate center point to the node position to the length of a straight line from the center point to the boundary passing through the node position. Another way to calculate R_c is by scaling the geometry in order that the node point falls in a boundary of the scaled plate, and the R_c is the square root of the area scale. Assuming the average value for the phase range described above, the approximated phase $\varphi_{1\mathrm{mod}}$ can then be described as:

$$\varphi_{1\,\mathrm{mod}} = arc\sin\left[\sin\left(\frac{\pi}{2}(1 - R_c)\right)\sin\left(\left(\frac{\pi}{2} + \frac{\pi}{2}(1 - R_c)\right)\frac{1}{2}\right)\right]. \tag{21}$$

2.4 Nodal acoustic source

The first attempt to include a nodal source in a volume to the use on SMM was like the implementation of the nodal force on a plate, however, as the eigenvector of a volume is dependent on wave counters that can assume the value zero, the equivalent ijn modal relation of volumes is not stable as the ij relation for plates (Eq. (18)); then, it was not possible to create a reasonable relation in this same way.

The modal nodal source was developed based on the high density of modes of acoustic systems. As acoustic systems have much more modes per band than the structural ones, the relevance of an individual mode losses importance compared to the global behavior of the band. Thus, for modal nodal source, the average of the eigenvector was applied, which resulted, respectively, in the equations below for the modal source, average module of eigenvector on volume interior, wall, edge and vertex:

$$Q_{m\_ijn}(x, y, z) = \frac{\int_V \hat{p}_{ijn}\delta(x, y, z)\frac{\partial q^2}{\partial t^2}\mathrm{d}V}{\int_V \hat{p}_{ijn}\hat{p}_{ijn}\mathrm{d}V} = \frac{\hat{p}_{ijn}(x, y, z)\frac{\partial Q^2}{\partial t^2}}{V_{ijn}} \cong \frac{\left|\bar{\hat{p}}_{ijn}\right|\frac{\partial Q^2}{\partial t^2}}{V_{ijn}} \tag{22}$$

$$\left|\bar{\hat{p}}_{ijn}\right| = \left[\int_0^{L_x}\cos^2\left(\frac{i\pi}{L_x}x\right)\frac{\mathrm{d}x}{L_x}\int_0^{L_y}\cos^2\left(\frac{j\pi}{L_y}y\right)\frac{\mathrm{d}y}{L_y}\int_0^{L_z}\cos^2\left(\frac{n\pi}{L_z}z\right)\frac{\mathrm{d}z}{L_z}\right]^{0.5} = \frac{1}{8^{0.5}} \cong 0.35 \tag{23}$$

$$\left|\bar{\hat{p}}_{ijn}\right| = \left[\int_0^{L_x}\cos^2\left(\frac{i\pi}{L_x}x\right)\frac{\mathrm{d}x}{L_x}\int_0^{L_y}\cos^2\left(\frac{j\pi}{L_y}y\right)\frac{\mathrm{d}y}{L_y}\right]^{0.5} = \frac{1}{4^{0.5}} = 0.5 \tag{24}$$

$$\left|\bar{\hat{p}}_{ijn}\right| = \left[\int_0^{L_x}\cos^2\left(\frac{i\pi}{L_x}x\right)\frac{\mathrm{d}x}{L_x}\right]^{0.5} = \frac{1}{2^{0.5}} \cong 0.7 \tag{25}$$

$$\left|\bar{\hat{p}}_{ijn}\right| = 1 \tag{26}$$

where Q_{m_ijn} is the modal source of mode ijn applied on position (x, y, z), and V_{ijn} is the modal volume. Additionally, it is considered that a point is on a volume vertex, edge or wall if its distance to these elements is smaller than $1/10$ of the acoustic wavelength in the applied frequency, in case of conflict it shall be used the higher value.

The proposed model works well on average for the interior and gets better as the node position gets close to the vertex due to the reduction on degrees of freedom.

2.5 Modal mass and volume

The last modal variables required for vibroacoustic analysis are the modal mass and volume. The modal mass of a rectangular plate has analytical solution, and therefore, it will be used on SMM:

$$
M_m = \rho \int_S w_m^2 \mathrm{d}s = \rho \left[\int_0^{L_x} \sin^2 \left(\frac{i\pi x}{L_x} \right) \mathrm{d}x \right]
$$
$$
\left[\int_0^{L_y} \sin^2 \left(\frac{j\pi y}{L_y} \right) \mathrm{d}y \right] = \rho \frac{L_x}{2} \frac{L_y}{2} = \frac{M_p}{4}
\tag{27}
$$

The modal volume requires more care on the calculations, as the wave counters on each direction of a rectangular volume can be zero, the modal volume results

$$
V_{ijn} = \left[\int_0^{L_x} \sin^2 \left(\frac{i\pi x}{L_x} \right) \mathrm{d}x \right] \left[\int_0^{L_y} \sin^2 \left(\frac{j\pi y}{L_y} \right) \mathrm{d}y \right]
$$
$$
\left[\int_0^{L_z} \sin^2 \left(\frac{n\pi z}{L_z} \right) \mathrm{d}z \right] = V \varepsilon_i \varepsilon_j \varepsilon_n
\tag{28}
$$

where $\varepsilon_x = 1$, for $x = 0$, and $\varepsilon_x = 1/2$, for $x > 0$.

Appealing again for the study with regular hexahedral volumes with aspect ratio varying from 1 to 10, it is possible to prove that the $\varepsilon_i \varepsilon_j \varepsilon_n$ for the first mode is always equal to 1, the second and third modes $\varepsilon_i \varepsilon_j \varepsilon_n$ are always equal to 0.5, from fourth to tenth modes the average result is 1/3, and thereafter, the average value of $\varepsilon_i \varepsilon_j \varepsilon_n$ is proportional to the relation $S^{1.5}/V$, as described in Eqs. (29–32) and Fig. 4.

$$
\varepsilon_i \varepsilon_j \varepsilon_n = 1, \text{ for fist mode}
\tag{29}
$$

$$
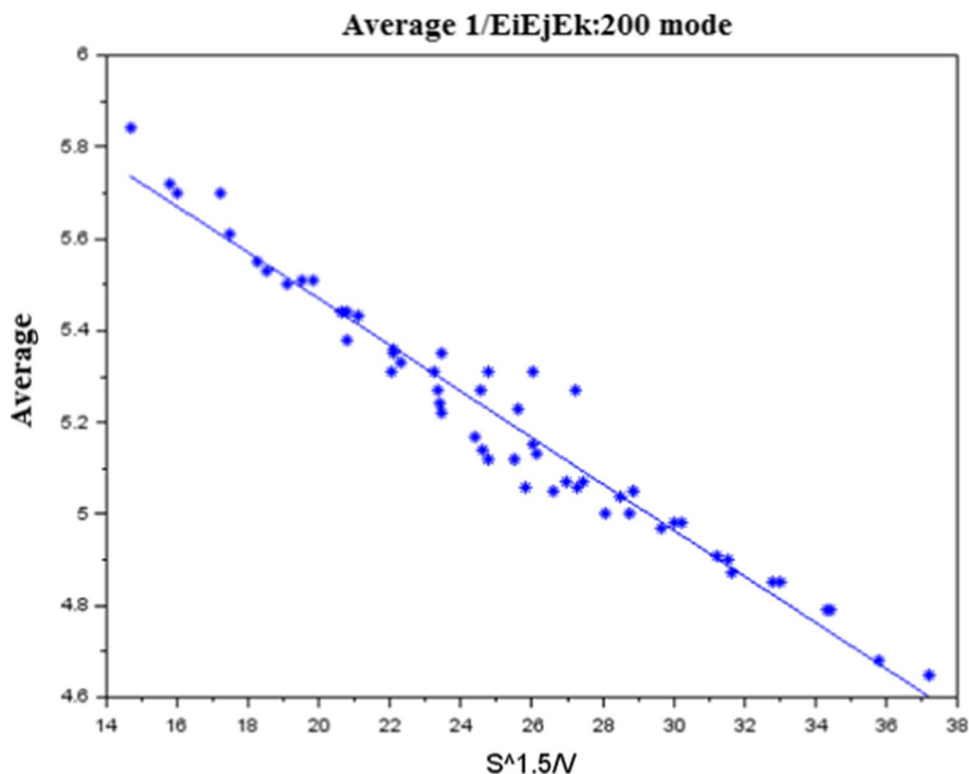\varepsilon_i \varepsilon_j \varepsilon_n = 0.5, \text{ for second and third modes}
\tag{30}
$$

$$
\varepsilon_i \varepsilon_j \varepsilon_n = 1/3, \text{ for fourth to tenth modes}
\tag{31}
$$

$$
\frac{1}{\varepsilon_i \varepsilon_j \varepsilon_n} = 6.477106 - 0.0504092 \frac{S^{1.5}}{V}, \text{ for others}
\tag{32}
$$

2.6 Coupled modal equations

From the literature, the coupled modal equations of a vibroacoustic problem are described according to

Fig. 4 $1/\varepsilon_i \varepsilon_j \varepsilon_n$ average of modes 11th to 200th in relation to the dimensionless relation $S.^1.5/V$ for rectangular volumes with aspect ratio from 1 to 10

$$\left(-\omega^2 + i\omega\left(2\alpha_{air}c + \frac{13.8}{T_{rev}}\right) + \omega_{ijn}^2\right)p_{ijn}$$
$$+ \omega^2 \frac{\rho c^2}{V_{ijn}} \sum_m \int_S \widehat{p}_{ijn}\widehat{w}_m \mathrm{d}S w_m \tag{33}$$
$$= \frac{c^2}{V_{ijn}} \int_V \hat{p}_{ijn} \frac{\partial^2 q}{\partial t^2} \mathrm{d}V$$

$$(-\omega^2 + 2i\zeta\omega_m\omega + \omega_m^2)w_m + \sum_{ijn} \int_S \widehat{p}_{ijn}\widehat{w}_m \mathrm{d}S \frac{p_{ijn}}{M_m} = \frac{1}{M_m} \int_S p\widehat{w}_m \mathrm{d}S \tag{34}$$

where the last term of left side of both equations is the coupling terms, α_{air} is the air absorption coefficient, T_{rev} is the reverberation time, and ξ is the plate damping coefficient.

The way used on SMM to keep the influence between mediums but decoupling the equations was to substitute couplings terms from Eqs. (33 and 34) to approximate couplings resistances derived specifically to simplify the response computations

$$\omega^2 \frac{\rho c^2}{V_{ijn}} \sum_m \int_S \widehat{p}_{ijn}\widehat{w}_m \mathrm{d}S w_m = -\omega^2 \frac{\rho c^2}{V_{ijn}} \sum_m \left[\frac{\left(\int_S \widehat{p}_{ijn}\widehat{w}_m \cdot \mathrm{d}S\right)^2}{M_m(-\omega^2 + 2i\zeta\omega_m\omega + \omega_m^2)}\right] p_{ijn} \tag{35}$$

$$\sum_{ijn} \int_S \widehat{p}_{ijn}\widehat{w}_m dS \frac{p_{ijn}}{M_m} = -\omega^2 \frac{\rho c^2}{M_m} \sum_{ijn} \left[\frac{\left(\int_S \widehat{p}_{ijn}\widehat{w}_m dS\right)^2}{V_{ijn}\left[-\omega^2 + i\omega\left(2\alpha_{ar}c + \frac{13.8}{T_{rev}}\right) + \omega_{ijn}^2\right]}\right] w_m \tag{36}$$

Equation (35) is calculated zeroing the terms of right side of Eq. (34) and isolating w_m, the same approach for Eq. (36).

2.7 Variable integral over frequency domain

The SMM evaluates the modal response of the variables which can be assumed to be also the maximum ones, as the eigenvectors used on SMM development are normalized in 1; then, the variables integral over frequency domain present the maximum result expected. However, it may be necessary to know the integral over some part of the domain, like volume interior, wall, edge and vertex or plate interior. For this purpose, it was used the statistical behavior of the method and adopted the average of the eigenvector module; thus, following the calculations of Eqs. (23–26), the integral

of the respective domains are equal to the integral of the obtained variable multiplied by: 0.35 for volume interior; 0.5 for volume wall and plate interior; 0.7 for volume edges; and 1 for vertex.

2.8 SMM implementation

The SMM implementation is simple and can be performed straightforward. First, the natural frequencies (Sect. 2.1), coupling factor (Sect. 2.2), modal input (Sects 2.3 and 2.4), modal mass and modal volume (Sect. 2.5) shall be evaluated based on geometrical data, material data, band frequency of interest and the excitation input of the system. Then, the modal summation shall be decoupled calculated following the equations of Sect. 2.6. In this sense, the decouple equations shall be solved sequentially following the load path. The subsystem which receives the input shall be solved first (Eq. 33 or 34) and considering the coupling resistances (Eq. 35 or 36) from the directly coupled subsystems, then the directly coupled subsystems shall be solved using the responses from the previous sub-

systems and accounting for coupling resistances of the next subsystems, and so on until the last coupled item of the load path.

As an example to clarify SMM implementation, consider an acoustic chamber excited by a loudspeaker (nodal source) with a plate mounted inside it. After evaluating all variables from Sects. 2.1–2.5, it is necessary to solve the modal equations according to the load path, first Eq. (33) shall be solved including the loudspeaker input and plate couple resistance from Eq. (35); then, after evaluating the pressure field, Eq. (34) shall be solved using the pressure field from last step as input (last term of left side of Eq. (34)).

The SMM works with modal summation, then, if more than one input is applied, it is just necessary to evaluate the responses for each input individually and sum the results.

3 SMM validation

The validation of the SMM method is performed in three ways: comparison with analytical results (Monte Carlo analysis with 864 interactions); comparison with numerical results obtained via FEM and SEA methods of the study of a car interior and a satellite inside a fairing and, finally, a comparison with experimental results obtained for the satellite Amazonia 1 acoustic test.

The analytical validation was used to develop the method and to provide statistical data regarding SMM error stats. The SMM development described in Sect. 2 was based in rectangular elements and, in that sense, a validation with non-rectangular shapes was mandatory, as presented in Sect. 3.2 with FEM and SEA. Finally, the SMM needed a real test data of a complex engineering case to assure its performance in real cases, and this is performed in Sect. 3.3 with Amazonia 1 satellite.

3.1 Analytical validation

The vibroacoustic process is of very high complexity, and therefore, it is not possible to define analytically the average and standard deviation errors of the SMM method. In order to overcome this issue, a Monte Carlo analysis with 864 interactions was performed. For all cases, rectangular volumes and plates were considered. The relative sizes, aspect ratios and plate positions varied for each case, half of the interactions were related to nodal force application and another half to nodal source. Table 2 presents the description of the cases used on the analysis.

The ratio of SMM integral of modal responses to the analytical integral of modal responses is presented in Fig. 5, where the averages varied from 1.3 to 2.2 and the standard deviation varied from 0.4 to 0.8. The ratio was better for the medium which received the input and some more error was propagated for the coupled medium, which is expected. For the medium which received the input a number of approximations were used, for the coupled medium

Table 2 Cases description of the Monte Carlo analysis

	Source input	Force input
Description	Panel mounted on side L_1L_2 of the volume with a source acoustic input, see Fig. 2	Panel with force input mounted on side L_1L_2 of the volume, see Fig. 2
Volume	2 m^3	2 m^3
Volumes aspect ratios	$L_1 \mid L_2 \mid L_3$: 1 | 1 | 1 1 | 2 | 3 2 | 1 | 2 3 | 1 | 2	$L_1 \mid L_2 \mid L_3$: 1 | 1 | 1 1 | 2 | 3 2 | 1 | 2 3 | 1 | 2
Plate aspect ratios	$L_{p1} \mid L_{p2}$: 1 | 1 1 | 2 3 | 1	$L_{p1} \mid L_{p2}$: 1 | 1 1 | 2 3 | 1
$(L_{p1}xL_{p2})/(L_1xL_2)$ and plate thickness	Ratio | Thickness: 0.7 | 10 mm 0.3 | 7 mm 0.05 | 3 mm	Ratio | Thickness: 0.7 | 10 mm 0.3 | 7 mm 0.05 | 3 mm
Input position	$P_{v1} \mid P_{v2} \mid P_{v3}$: 0 | 0 | 0 $L_1/8 \mid L_2/8 \mid L_3/8$ $L_1/4 \mid L_2/4 \mid L_3/4$ $L_1/2 \mid L_2/2 \mid L_3/2$	$P_{p1} \mid P_{p2}$: $L_{p1}/4 \mid L_{p2}/2$ $L_{p1}/2 \mid L_{p2}/4$ $L_{p1}/4 \mid L_{p2}/4$ $L_{p1}/2 \mid L_{p2}/2$
Panel position (bottom left point)	$P_1 \mid P_2$: 0 | 0 | 0 $L_1/4 \mid L_2/4$ $L_1/2 \mid L_2/2$	$P_1 \mid P_2$: 0 | 0 $L_1/4 \mid L_2/4$ $L_1/2 \mid L_2/2$

(a)

Modal Acceleration
Average = 2.02 / SD = 0.58

(c)

Modal Acceleration
Average = 1.53 / SD = 0.39

(b)

Modal Pressure
Average = 1.33 / SD = 0.41

(d)

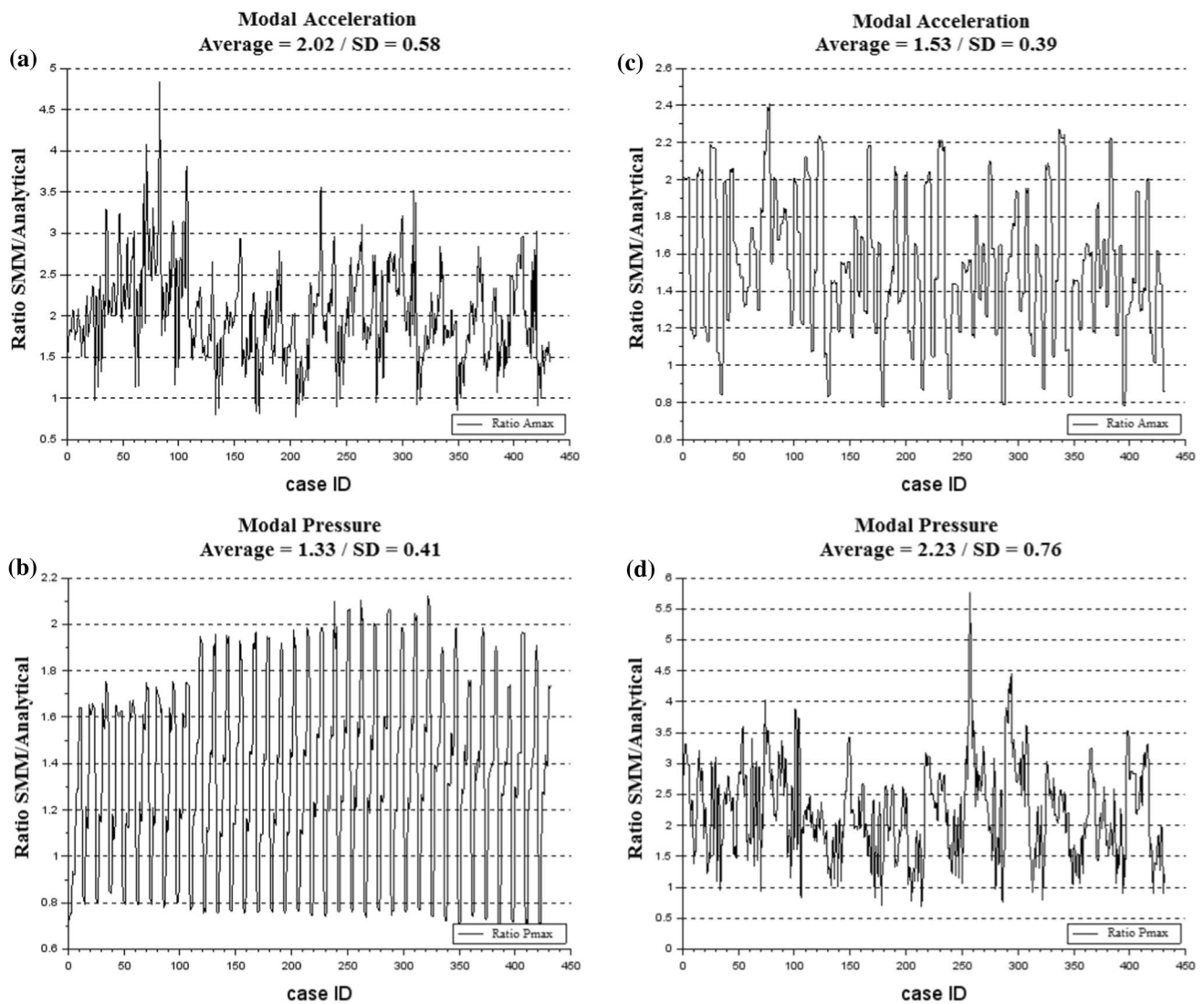**Modal Pressure**
Average = 2.23 / SD = 0.76

Fig. 5 Ratio of SMM integral responses to the analytical integral responses for the 864 Monte Carlo interactions: **a** and **b** source input; **c** and **d** force input

the approximations necessary for its evaluations are the ones used in the input medium plus the coupling factor approximations and the medium itself approximations. The results were a little better for the source input, because as the volume has much more modes than the plate, the errors in the natural frequency estimator were minimized. The degree of accuracy of the method can be considered adequate and reliable, the integral variations allow a proper design of coupled systems, as it represents a relative energy variation acceptable for phases pre-experimental tests, where a calibration on stiffness and damping can adjust the model, additionally, the maximum responses, as shown on some examples of Fig. 6, are all captured within the same order of magnitude, these values will mostly dictate the analysis of strength and dynamic compatibility of the elements, by example, of electronic equipment mounted in a satellite panel.

3.2 FEM and SEA validation

The SMM was designed and validated in last sections based on rectangular elements with analytical solution. Thus, it is mandatory to also validate the method for cases with non-rectangular geometries and representative as vibroacoustic systems. Two cases were designed to fulfill these requirements: a car interior and a satellite inside a fairing.

3.2.1 Car interior case

A simplified model of a car with a single seat and window was considered and is described in Fig. 7, the model total volume is 0.0117 m³ and fulfilled with air. The plate area is 0.0103 m², and it is constituted by aluminum 8-mm thick. A harmonic nodal force of 10 N is applied at the plate
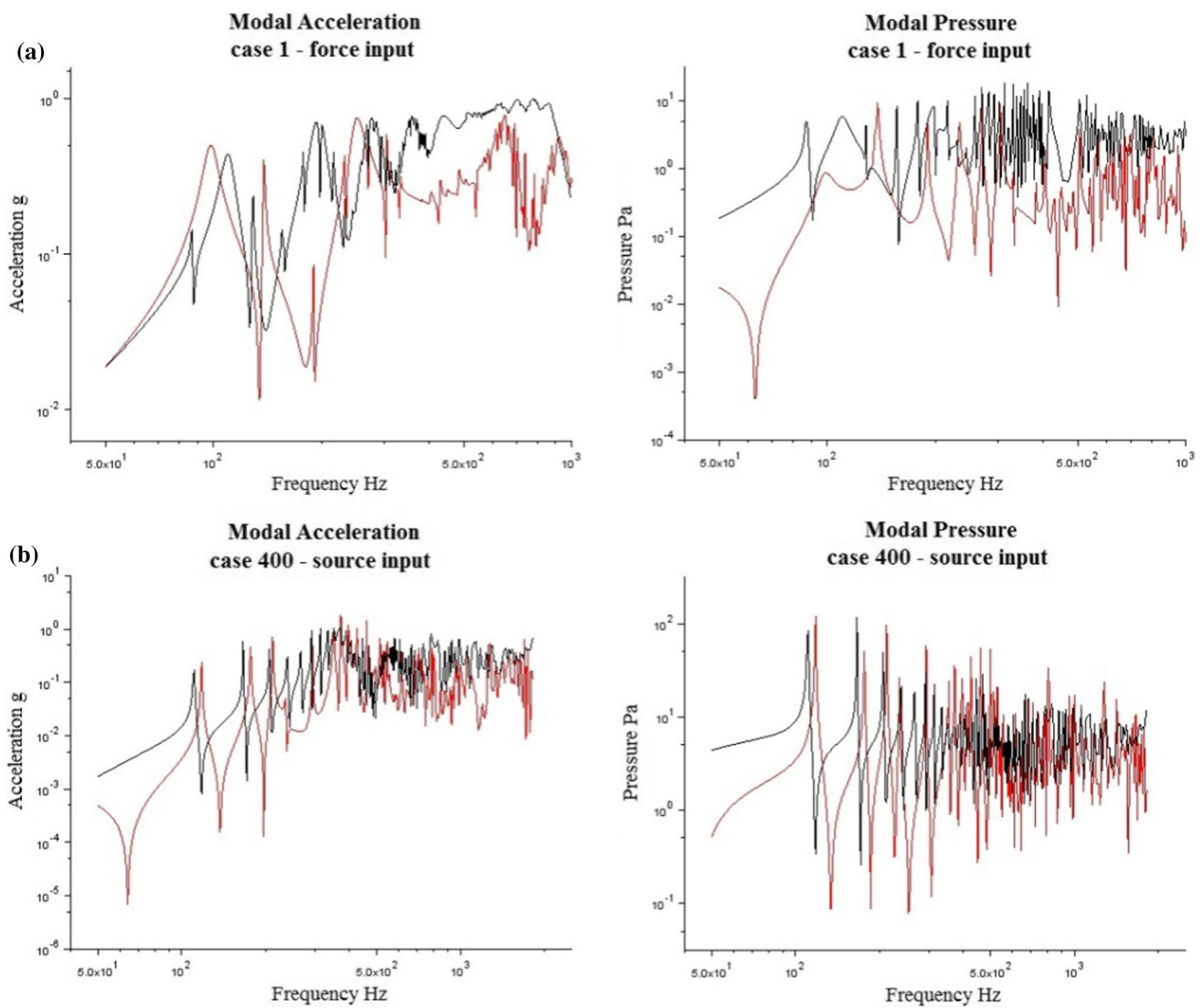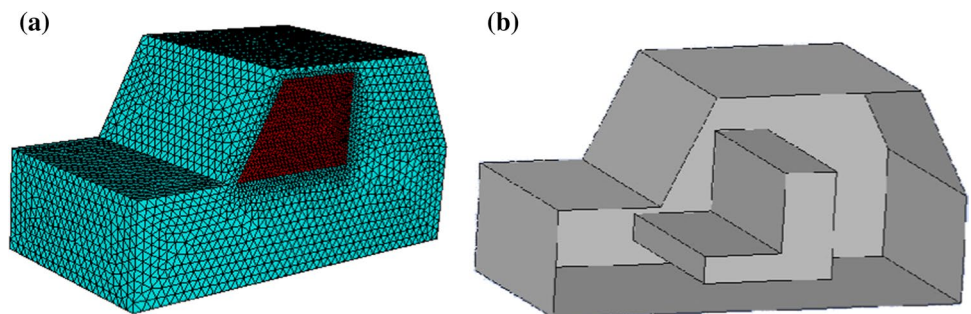
Fig. 6 Modal responses comparison of SMM (black) to analytical results (red): **a** Case 1—force input; **b** case 400 – source input

Fig. 7 Car interior case with plate (window) in red: **a** mesh; **b** internal geometry (car geometry fits in a box 0.4×0.2×0.2 m)

center, and its frequency varies over the frequency band from 50 to 5,000 Hz. The FEM analysis was run in Elmer, an open-source multiphysical software [26], using a mesh with 12,762 nodes, 57,548 volume acoustic elements and 1468 plate elements. The maximum responses obtained from FEM, SEA and SMM were compared and are plotted in Fig. 8. Elmer software solves the finite element matrix numerically for every frequency; the total run time for Elmer FEM was 4366 s. The SMM took 53 s to solve the problem in the same frequencies. In addition to the computational
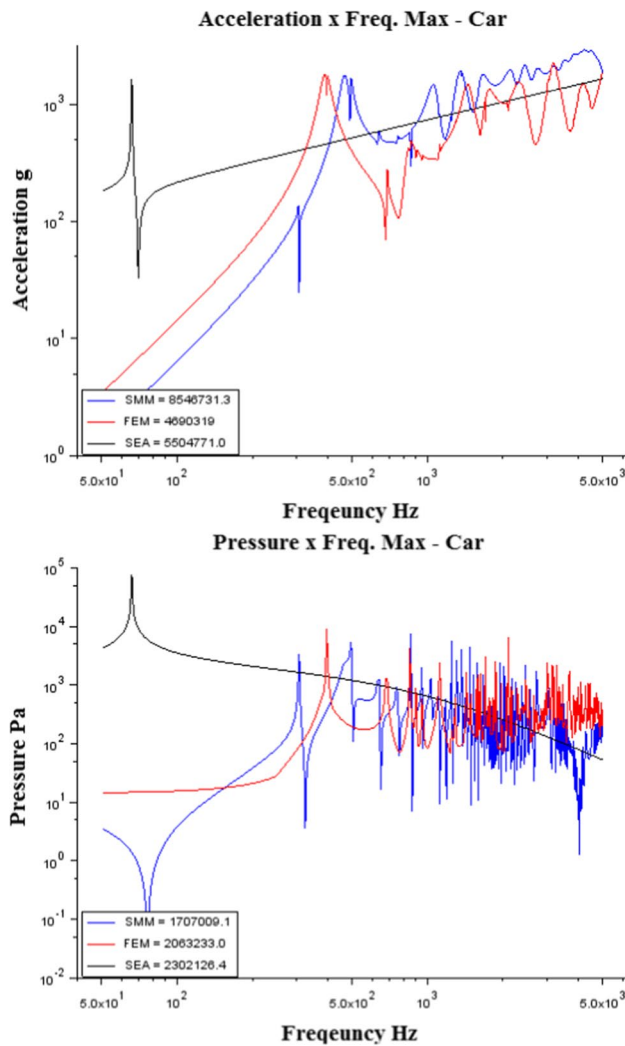
Fig. 9 Satellite in fairing case with plate (antenna) in red: Two views (faring fits in a cubic box of 0.2 m)

3.2.2 Satellite in fairing case

A simplified model of a satellite inside a fairing is now considered. The fairing geometry is approximated as a cylindrical volume with a semi-sphere on the top, while the satellite is modeled as squared cut extrusion in the center of the cylinder. On the satellite top is placed an elliptical antenna which is modeled as the plate of this model. The fairing interior volume is 0.0042 m^3 (fulfilled with air), and the antenna area is 0.0025 m^2. The antenna is an aluminum plate 4 mm thick. A harmonic source of 10 kg/s^2 from 5 to 5,000 Hz was applied at the cylinder center line above the antenna position. The FEM model mesh is displayed in Fig. 9 and has 4,209 nodes, 17,421 volume acoustic elements and 285 plate elements. The maximum results from FEM were plotted with results from SMM and SEA in Fig. 10 for comparison purposes. SMM could capture with good agreement to FEM the maximum responses on each frequency band and the integral over the frequency ratio from SMM to FEM is 2.1 for acceleration and 0.9 for pressure, which is in agreement with analytical errors showed in Sect. 3.1. In this case, as the fairing has an axis of symmetry, there are much more degenerate modes and for that reason the SMM shows more modes per band than FEM, see Fig. 10. SEA captured the average behavior but was not capable to deal with maximum responses and lower frequencies close to the first modes, as in car cabin case. The FEM responses were computed with Elmer software [26] and the total run time was 564 s, while the SMM executed the results in 8 s. The processing time difference shows the low computational cost of SMM; another relevant point is related to the time spent building the mesh and finite element model, which is not necessary on SMM.

The results obtained for the two presented models showed the potential of the method even in more complex geometries. The maximum frequencies were well captured, and

Fig. 8 Acceleration and pressure maximum responses in the car interior case. SMM in blue, SEA in black and FEM in red

efficiency, it is necessary to take into account the necessary time to build the mesh and configure it in the solver, while in SMM, it is only necessary to fulfill the systems properties, such as area, volume, and material data.

SMM could describe with very good accuracy the maximum responses of pressures in the cavity and acceleration in the plate in all frequency spectrum; the error of maximum magnitude around the first mode of each subsystem is 38% for pressure and 2% for acceleration. The SMM integral ratio to FEM was 0.8 for pressure and 1.8 for acceleration. SEA presented only the average response with good integral estimation, but was not capable to capture the maximum responses and overestimated results below 300 Hz.
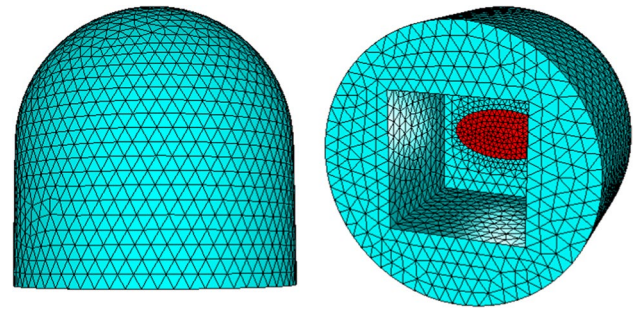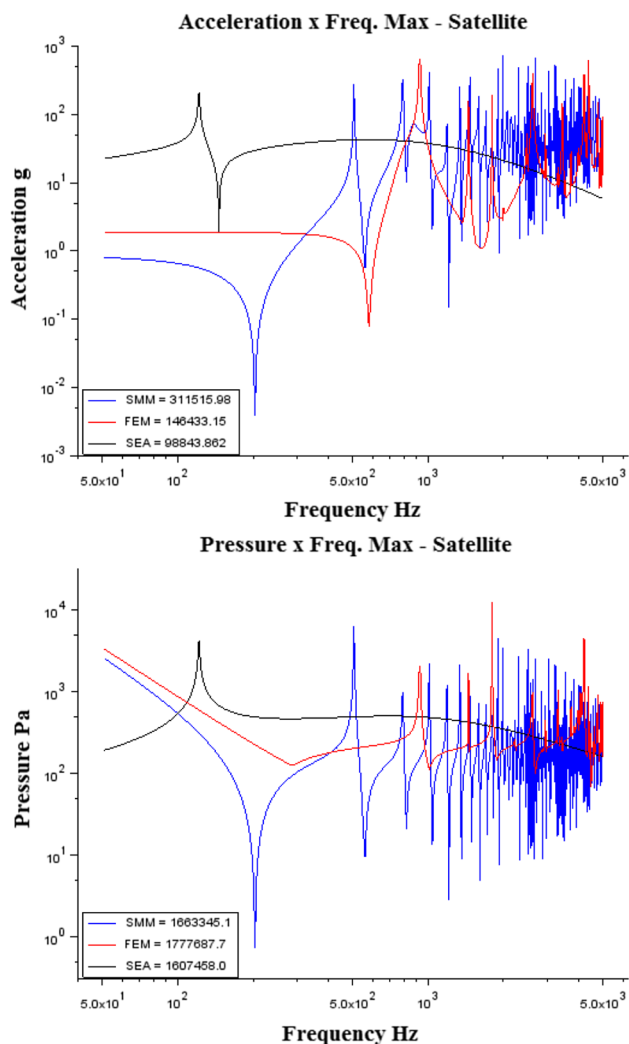
Fig. 10 Acceleration and pressure maximum responses in the satellite inside fairing case. SMM in blue, SEA in black and FEM in red

Fig. 11 Amazonia 1 satellite inside acoustic chamber (*Source*: INPE)

The mission provides images in green, blue, red and NIR (near infrared) bands with resolution of around 65 m on nadir. For the tests, the satellite was mounted in a special trolley isolated from the ground and positioned inside a chamber with $10.5 \times 8.4 \times 20$ m in an oblique way to its walls, four control microphones were positioned in the satellite center one meter from its lateral panels, as showed in Fig. 11. The INPE's acoustic chamber is a closed loop reverberant chamber where high-pressure gaseous nitrogen

the integrals over the frequency domain presented similar results to the ones obtained for the Monte Carlo analysis with rectangular geometries. This validates the results to be applied in a wide range of problems. The SMM seems to present more information than SEA and is close to FEM results.

3.3 Experimental validation

The last and more important validation of SMM is against Amazonia 1 satellite acceptance tests. The Amazonia 1 satellite is a project from INPE and passed through acoustic tests in the middle of 2020 in order to be accepted for launch, which happened in February of 2021 by a PSLV rocket. Amazonia 1 is a satellite with around 640 kg. It was designed for a sun-synchronous orbit with approximately 750 km height and equatorial passage of 10:30 h.
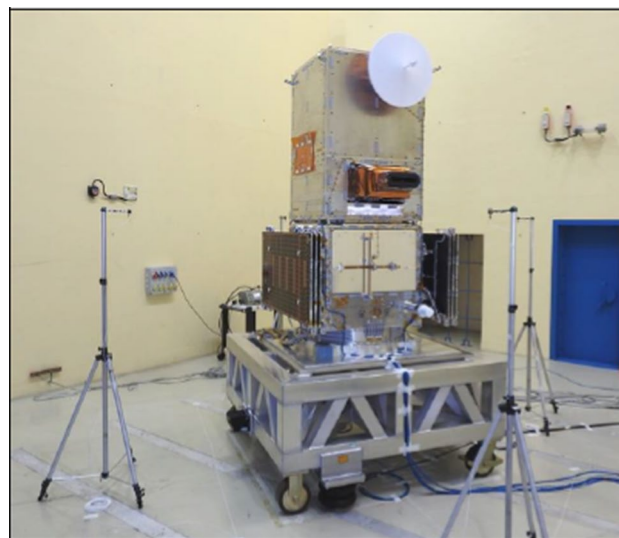
Table 3 Pressure field registered during Amazonia 1 acceptance test, frequency defined in 1/3 octave (Source: INPE)

Frequency (Hz)	SPL (dB)	Frequency (Hz)	SPL (dB)
31.5	123.88	1000	135
63	126.16	2000	126.66
125	129.65	4000	120.78
250	135.82	8000	119.57
500	139.81	OASPL	142.75

Table 4 SMM and tests results Grms (Source: INPE)

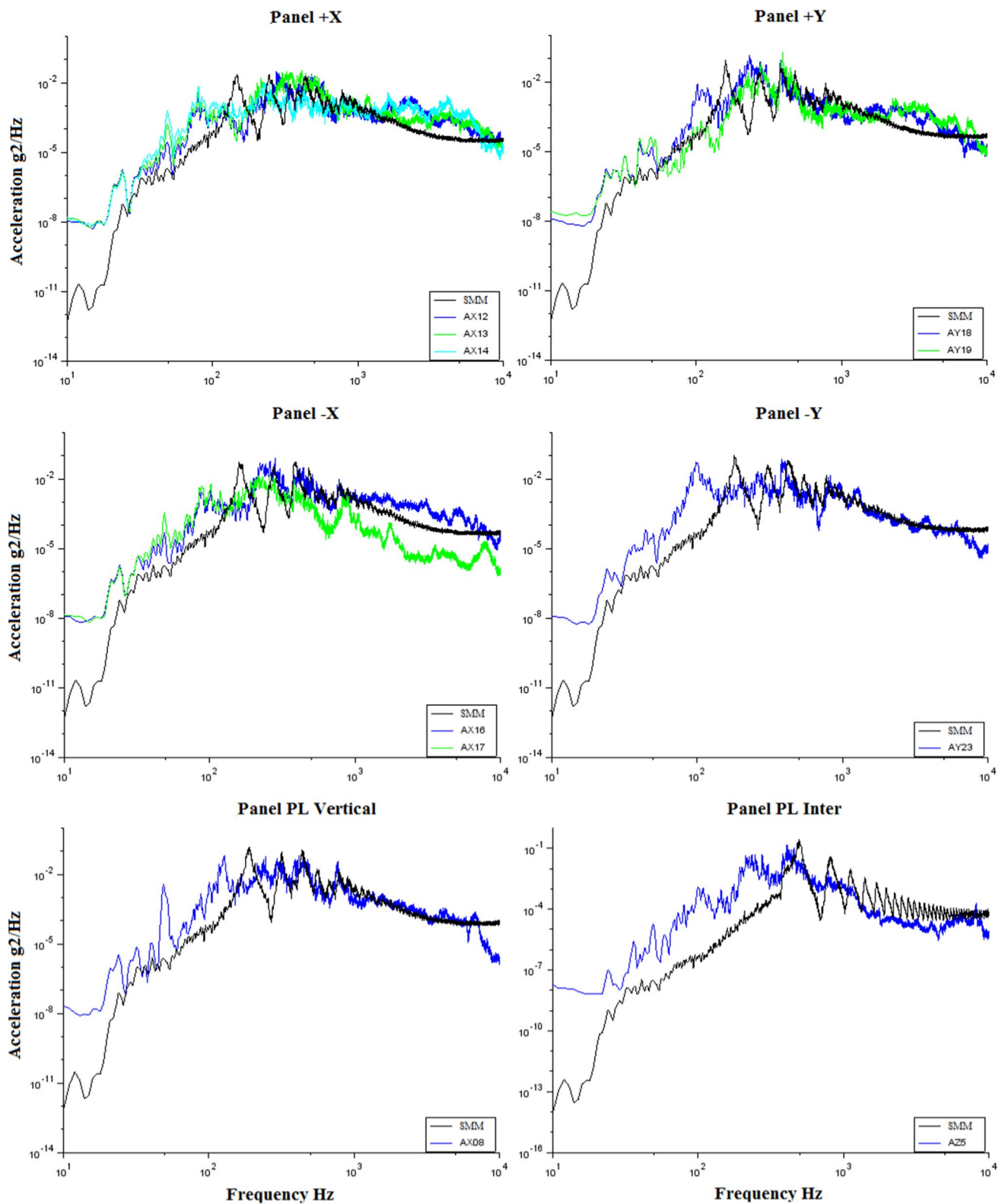| Panel	SMM Grms	Test Grms	Ratio SMM/Test
+X	1.78	2.34	0.76
+Y	2.23	2.73	0.82
-X	2.33	2.01	1.16
-Y	2.77	2.45	1.13
PL vert	3.23	3.11	1.04
PL inner	3.55	2.84	1.25

Fig. 12 SMM validation to Amazonia 1 satellite acoustic tests, SMM in black (*Source*: INPE)
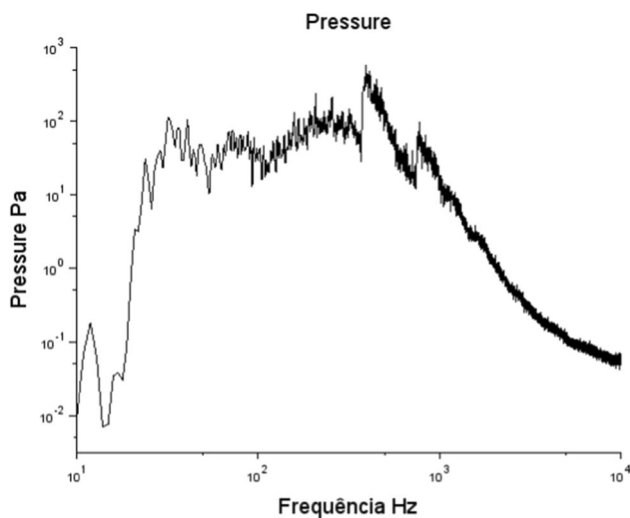
Fig. 13 Amazonia 1 satellite acoustic tests: Microphones pressure average (*Source*: INPE)

is used to generate high-intensity noise by means of gas stream modulators connected to horns placed in the chamber's top. The specified pressure field is monitored by the control microphones. The acceptance tests are preceded by functional electrical tests and signature pressure tests, which has a pressure field 6 dB lower than acceptance test itself. Then, after the acceptance test, these two verifications are repeated and compared with the initial ones. The registered pressure obtained during the test is showed in Table 3.

The accelerations recorded in the satellite six different panels were used as reference data to validate the SMM. Amazonia 1 panels are sandwich panels with honeycomb and face sheet of aluminum. Considering yet that SMM frequency estimator only accounts for bending modes, sandwich panels have much more modes in high frequencies than a homogeneous plate and taking advantage on SEA heritage, which calculates the coupled response to be direct proportional to the modes density, a corrector factor equal to the ratio of sandwich panels modes density to normal homogenous panels modes density was applied, what seemed to be very relevant to improve the accuracy of the approximation in higher frequencies. The sandwich panel modal density formula was taken from Wijker [24]

$$n_{\mathrm{est}}(f) = \frac{2\pi f S}{c_{\mathrm{b,eff}}^2}\left(1 - \frac{\left[\frac{1}{c_{\mathrm{b}}^3} + \frac{1}{c_{\mathrm{s}}^3}\right]^{-4/3}}{2c_{\mathrm{b,eff}}c_{\mathrm{b}}^3}\right) \tag{37}$$

where c_{b} is the bending wave speed, c_{s} is the shear wave speed, and $c_{\mathrm{b,eff}}$ is the effective bending wave speed.

The results of SMM and test measurements are presented in Table 4 and Fig. 12, it can be noted that the maximum acceleration on each frequency band is very close, the global behavior and tendencies are well captured, and finally, the Grms responses are in good agreement, the Grms ratio from SMM to test data varied from 0.76 to 1.25.

The SMM results detached from the experimental ones in frequencies below 25 Hz. In fact, at these frequencies, the input pressure had a drop down (Fig. 13), which was captured by the SMM, and however, the panels still presented some response in the test. This may be caused by lower frequencies interactions to the satellite and satellite trolley, both not modeled in the SMM model used.

4 Conclusions

A novel method for vibroacoustic coupled analyses was developed, the statistical modes method — SMM. The method is based on the calculus of eigenvalues from modified modal density equations and provides two main outputs, the maximum responses over each frequency band and the overall responses through the integral over the frequency domain. The SMM seems to be a method with simple implementation and low computational cost that can solve a coupled system in a statistical way, presenting reasonable results for all frequency bands. The method was validated by analytical models, by FEM, by SEA and by experimental data from Amazonia 1 satellite acceptance tests. In all cases, the maximum responses were well captured and the integrals obtained were in average around 1.3–2.2 times the real ones, which is sufficient accuracy for analysis before the execution of physical tests, usually used to tune the model. The SMM seems to provide more information than SEA with not much more computation effort, in this sense is a method much more simple than FEM but not too much complicated than SEA.

A significant part of the errors obtained by the proposed method on the integrals or maximum responses calculations can be regarded to the degraded modes, which are not yet modeled by the SMM method. As part of future developments, an algorithm is planned to take into account degraded modes in symmetrical elements.

The objective of creating a method with low computational cost that provides reasonable accuracy in low, medium and high frequencies for coupled vibroacoustic systems has been achieved. The presented results show that the SMM can be used in several vibroacoustics coupled analysis with consistent results.

Declarations

Conflict of interest The authors have no competing interests to declare that are relevant to the content of this article.

References

1. Desmet W, Pluymers B, Atak O (2008) Mid frequency—cae methodologies for mid-frequency analysis in vibration and acoustics. Eur FP7 Marie Curie Initial Train Netw (ITN)
2. Langley R, Cordioli J (2009) A hybrid deterministic-statistical analysis of vibro-acoustic systems with domain couplings on statistical components. J Sound Vib 192(1):483–500
3. Pirk R, Souto CA (2015) Deterministic, hybrid and statistical vibro-acoustic models—A methodology to determine the VLS payload fairing acoustic behavior. J Aerosp Technol Manag 7:101–109
4. Jiao R, Nguyen V, Zhang J (2020) Acoustic-structure modeling and analysis of an engineering machinery cab based on the hybrid method and experimental investigations. J Braz Soc Mech Sci Eng 42:1–8
5. Desmet WA (1998) Wave-based prediction technique for coupled virbo-acoustic analysis. Thesis (PhD)–Katholiek Universiteit Leuven
6. Desmet W, Hal B, Sas P, Vandepitte D (2002) A computationally efficient prediction technique for the steady-state dynamic analysis of coupled vibro-acoustic systems. Adv Eng Softw 33:527–540
7. Hal B, Desmet W, Vandepitte D (2003) A coupled finite element-wave based approach for the steady-state dynamic analysis of acoustic systems. Int Assoc Math Comput Simul 11:285–303
8. Vanmaele C (2007) Development of a wave based prediction technique for the efficient analysis of low- and mid-freqency structural vibrations. Thesis (PhD)–Katholiek Universiteit Leuven
9. Stelzer R (2012) An energy based method for coupled vibro-acoustic systems. Thesis (PhD)–INSA Lyon
10. Stelzer R, Totaro N, Pavic G, Guyader JL (2012) Application of SmEdA to systems with high mode densities. In: proceedings of conference noise and vibrations emerging methods
11. Braz BC, Souto CA (2021) Acoustic vibration environment prediction for Amazonia 1 satellite using SEA method. CILAMCE-PANACM
12. Anvariyeh FS, Jalili MM, Fotuhi AR (2019) Nonlinear vibration analysis of a circular plate-cavity system. J Braz Soc Mech Sci Eng 41(2):1–13
13. Zhong R, Guan X, Wang W, Qin B, Shuai C (2021) Prediction of acoustic radiation from elliptical caps of revolution by using a semi-analytic method. J Braz Soc Mech Sci Eng 43(8):1–17
14. Fahy FJ (1994) Statistical energy analysis: a critical overview. Philos Trans: Phys Sci Eng 346:431–447
15. Bolt RH (1939) Normal modes of vibration in room acoustics: Experimental investigations in nonrectangular enclosures. J Acoust Soc Am 11:14
16. Bolt RH (1946) Note on normal frequency statistics for rectangular rooms. J Acoust Soc Am 18:4
17. Bolt RH (1947) Normal frequency spacing statistics. J Acoust Soc Am 19:12
18. Schroeder MR, Kuttruff KH (1962) On frequency response curves in rooms. comparison of experimental, theoretical, and Monte Carlo results for average frequency spacing between maxima. J Acoust Soc Am 34(76):5
19. Bonello OJ (1981) A new criterion for the distribution of normal modes. J Audio Eng Soc 29(9):597–606
20. Cox TJ, D'Antonio P, Avis MR (2004) Room sizing and optimization at low frequencies. J Audio Eng Soc 52(6):640–651
21. Hart FD, Shah KC (1971) Compendium of modal densities for structures. NASA, NASA CR-1773
22. Clarkson BL, Ranky MF (1983) Modal density of honeycomb plates. J Sound Vib 91(1):103–118
23. Xie G, Thompson DJ, Jones CJC (2004) Mode count and modal density of structural systems: Relationships with boundary conditions. J Sound Vib 247:621–651
24. Wijker J (2009) Random vibration in spacecraft structures design. Springer, Newyork
25. Wolfram Alpha Homepage, http://www.wolframalpha.com, last accessed 2021/11/20
26. Elmer FEM Homepage, http://www.emerfem.org, last accessed 2021/11/20